UC San Diego
UC San Diego Previously Published Works

Title

Role of KCC2-dependent potassium efflux in 4-Aminopyridine-induced Epileptiform synchronization

Permalink

Journal

ISSN

Authors

González, Oscar C
Shiri, Zahra
Krishnan, Giri P
et al.

Publication Date

DOI

Peer reviewed

Role of KCC2-Dependent Potassium Efflux in 4-Aminopyridine-Induced Epileptiform Synchronization

Oscar C González[1,2], **Zahra Shiri**[3], **Giri P Krishnan**[2], **Timothy L Myers**[6,7], **Sylvain Williams**[4], **Massimo Avoli**[3,5], and **Maxim Bazhenov**[1,2]

[1]Neurosciences Graduate Program, University of California, San Diego, CA

[2]Department of Medicine, University of California, San Diego, CA

[3]Montreal Neurological Institute, McGill University, Montréal, H4H 1R3 Québec, Canada

[4]Douglas Mental Health University Institute, McGill University, Montréal, H4H 1R3 Québec, Canada

[5]Department of Physiology, McGill University, Montréal, H4H 1R3 Québec, Canada

[6]Neuroscience Graduate Program, University of California, Riverside, CA

[7]Department of Cell Biology and Neuroscience, University of California, Riverside, CA

Abstract

A balance between excitation and inhibition is necessary to maintain stable brain network dynamics. Traditionally, seizure activity is believed to arise from the breakdown of this delicate balance in favor of excitation with loss of inhibition. Surprisingly, recent experimental evidence suggests that this conventional view may be limited, and that inhibition plays a prominent role in the development of epileptiform synchronization. Here, we explored the role of the KCC2 co-transporter in the onset of inhibitory network-induced seizures. Our experiments in acute mouse brain slices, of either sex, revealed that optogenetic stimulation of either parvalbumin- or somatostatin-expressing interneurons induced ictal discharges in rodent entorhinal cortex during 4-aminopyridine application. These data point to a proconvulsive role of $GABA_A$ receptor signaling that is independent of the inhibitory input location (i.e., dendritic *vs.* somatic). We developed a biophysically realistic network model implementing dynamics of ion concentrations to explore the mechanisms leading to inhibitory network-induced seizures. In agreement with experimental results, we found that stimulation of the inhibitory interneurons induced seizure-like activity in a network with reduced potassium A-current. Our model predicts that interneuron stimulation triggered an increase of interneuron firing, which was accompanied by an increase in the intracellular chloride concentration and a subsequent KCC2-dependent gradual accumulation of the extracellular potassium promoting epileptiform ictal activity. When the KCC2 activity was

To whom correspondence should be addressed: Maxim Bazhenov, Department of Medicine, University of California, San Diego, La Jolla, CA 92093, Phone: 858-534-8391, mbazhenov@ucsd.edu.

Conflicts of interest: none.

reduced, stimulation of the interneurons was no longer able to induce ictal events. Overall, our study provides evidence for a proconvulsive role of $GABA_A$ receptor signaling that depends on the involvement of the KCC2 co-transporter.

1. Introduction

Under specific conditions, activation of the inhibitory $GABA_A$ receptor signaling may play a prominent role in the generation of seizures (Lillis et al., 2012; Hamidi and Avoli, 2015; Sessolo et al., 2015; Uva et al., 2015; Yekhlef et al., 2015; Shiri et al., 2016). This evidence is in conflict with the established notion that epileptiform discharges result from excessive glutamatergic signaling due to reduced inhibition (Ben-Ari et al., 1979; Dingledine and Gjerstad, 1980; Schwartzkroin and Prince, 1980). Indeed, it has been shown that inhibitory interneurons discharge action potentials at the onset of seizure-like events both *in vitro* (Lillis et al., 2012; Uva et al., 2015; Levesque et al., 2016) and *in vivo* (Grasse et al., 2013; Toyoda et al., 2015). Moreover, seizure-like discharges *in vitro* disappear after pharmacological interventions that interfere with $GABA_A$ receptor signaling (Avoli et al., 1996; Lopantsev and Avoli, 1998; Uva et al., 2015). In line with this evidence, direct optogenetic activation of inhibitory interneurons during bath application of 4-aminopyridine (4AP) elicits seizure-like discharges *in vitro* (Yekhlef et al., 2015; Shiri et al., 2016). Together, these data suggest that an increase in the inhibitory interneuron synchrony may lead to development of paroxysmal seizure-like activity under conditions of impaired potassium (K^+) channel conductances. However, the mechanisms of this action remain to be fully understood.

Intracellular chloride concentration ($[Cl^-]_i$) increases in principal neurons at the onset of seizure-like activity in 4AP treated conditions (Lillis et al., 2012). Such intracellular accumulation of $[Cl^-]_i$, which is presumably due to an increase in GABAergic signaling prior to seizure onset, can be accompanied by a large increase in the extracellular potassium concentration ($[K^+]_o$) (Krishnan and Bazhenov, 2011). *In vitro* optogenetic stimulation of inhibitory interneurons can increase $[K^+]_o$ to the level capable of inducing seizure-like discharges (Yekhlef et al., 2015). An elevated level of $[K^+]_o$ may function as a positive feedback loop, increasing overall network excitability and leading to seizure onset (Pedley et al., 1974; Traynelis and Dingledine, 1988; Somjen, 2002; Frohlich and Bazhenov, 2006; Frohlich et al., 2008; Krishnan and Bazhenov, 2011; González et al., 2015). Indeed, fast-rising $[K^+]_o$ increases associated with interneuronal network activity preceded the initiation of seizure-like events *in vitro* in the 4AP seizure model (Librizzi et al., 2017). Previous computational studies found that oscillations of $[K^+]_o$ mediate periodic transitions between fast runs and spike-and-wave complexes during seizures (Frohlich and Bazhenov, 2006; Frohlich et al., 2008; Krishnan and Bazhenov, 2011), and that increase in baseline $[K^+]_o$ fluctuations may occur following cortical trauma (González et al., 2015). K^+ dynamics have

been implicated in the transition to seizure and spreading depression (Wei et al., 2014), two network states previously thought to be mechanistically distinct.

The potassium-chloride co-transporter isoform 2 (KCC2) has been proposed as the critical link between the increase in $[Cl^-]_i$ and subsequent increase in $[K^+]_o$ (Rivera et al., 2005; Hamidi and Avoli, 2015; Shiri et al., 2016). Indeed, reduction of KCC2 activity prevents generation of seizure-like events induced by 4AP (Hamidi and Avoli, 2015), as well as the increases in $[K^+]_o$ that occur in response to high-frequency stimulation (Viitanen et al., 2010). Therefore, it was postulated that synchronized GABAergic activity may cause a gradual accumulation of $[Cl^-]_i$, leading to the activation of KCC2. This results in the extrusion of both Cl^- and K^+, allowing K^+ to reach the level necessary to elicit seizure (Avoli and de Curtis, 2011; Avoli et al., 2016).

In our new study, we tested this hypothesis by employing biophysically realistic network model with dynamic ion concentrations, Na^+/K^+ ATPase activity, and KCC2 activity. We found that reduction of the outward K^+ (type A) current (I_A), mimicking the effects of 4AP application, changed the network dynamics so interneuron stimulation could initiate seizure-like activity. Importantly, reduction of KCC2 activity (*cf.*,(Hamidi and Avoli, 2015)) prevented seizure generation, thus supporting our hypothesis about the role of KCC2 in ictogenesis.

2. Methods

2.1. Animals

All procedures were performed according to protocols and guidelines of the Canadian Council on Animal Care and were approved by the McGill University Animal Care Committee. PV-Cre (Jackson Laboratory, B6;129P2-*Pvalb^{tm1(cre)Arbr}*/J, stock number 008069) and SOM-Cre (Jackson Laboratory, *Ssttm2.1(cre)Zjh*/J, stock number 013044) homozygote mouse colonies were bred and maintained in house in order to generate pups that were used in this study.

2.2. Stereotaxic virus injections

Four PV-Cre (2 male and 2 female) and five SOM-Cre (3 male and 2 female) pups were anesthetized at P15 using isoflurane and positioned in a stereotaxic frame (Stoelting). AAVdj-ChETA-eYFP virus (UNC Vector Core) was delivered in the entorhinal cortex (EC) (0.6 μL at a rate of 0.06 μL/min). Injection coordinates were: anteroposterior −4.00 mm from bregma, lateral +/− 3.60 mm, dorsoventral −4.00 mm. The transverse sinus was used as a point of reference, and the injection needle was inserted with a 2° anteroposterior angle. After completion of the surgery, pups were returned to their home cage.

2.3. Brain slice preparation

Mice were deeply anesthetized with inhaled isoflurane and decapitated at P30–40. Brains were quickly removed and immersed in ice-cold slicing solution containing (in mM): 25.2 sucrose, 10 glucose, 26 $NaHCO_3$, 2.5 KCl, 1.25 KH_2PO_4, 4 $MgCl_2$, and 0.1 $CaCl_2$ (pH 7.3, oxygenated with 95% O_2/5% CO_2). Horizontal brain sections (thickness = 400 μm)

containing the EC were cut using a vibratome (VT1000S, Leica) and incubated for one hour or more in a slice saver filled with artificial cerebrospinal fluid (ACSF) of the following composition (in mM): 125 NaCl, 25 glucose, 26 $NaHCO_3$, 2 KCl, 1.25 NaH_2PO_4, 2 $MgCl_2$, and 1.2 $CaCl_2$.

2.4. Electrophysiological recordings, photostimulation, and analysis

Slices were transferred to a submerged chamber where they were continuously perfused with oxygenated ACSF (KCl and $CaCl_2$ adjusted to 4.5 and 2 mM, respectively) (30 °C, 10–15 mL/min). Field potentials were recorded using ACSF-filled microelectrodes (1–2 MΩ) positioned in the EC in the presence of 4AP (150 μM). Signals were recorded with a differential AC amplifier (AM systems), filtered online (0.1–500 Hz), digitized with a Digidata 1440a (Molecular Devices) and sampled at 5 kHz using the pClamp software (Molecular Devices).

For ChR2 excitation, blue light (473 nm, intensity 35 mW) was delivered through a custom-made LED system, where the LED (Luxeon) was coupled to a 3 mm wide fiber-optic (Edmund Optics) and was placed above the recording region. For optogenetic stimulation of interneurons, light pulses (1 s duration) were delivered at 0.2 Hz for 30 s with a 150 s interval between trains. All reagents were obtained from Sigma-Aldrich and were bath applied. Ictal duration and interval are expressed as mean ± SEM. Data were compared using the Student's t-test. Results were considered significant if the p-value was less than 0.05.

2.5. Principal neuron and interneuron models

Principal or excitatory neurons (PNs) and inhibitory interneurons (INs) were both modeled as two compartment models as described previously in (Bazhenov et al., 2002, 2004; Houweling et al., 2005; Frohlich et al., 2008; Krishnan and Bazhenov, 2011; Volman et al., 2011a; Volman et al., 2011b; González et al., 2015; Krishnan et al., 2015). The membrane potential dynamics for each compartment were modeled by the following equations:

$$C_m \frac{dV_D}{dt} = -g_D^c (V_D - V_S) - I_D^{leak} - I_D^{pump} - I_D^{Int}$$
$$g_S^c (V_D - V_S) = -I_S^{leak} - I_S^{pump} - I_S^{Int}$$

where $V_{D,S}$ are the dendritic and axosomatic membrane potentials, $g_{D,S}^c$ are the dendritic and axosomatic compartment coupling current conductance, I_D^{pump} and I_S^{pump} are the sum total Na^+/K^+ ATPase currents, I_D^{leak} and I_S^{leak} are the sum of the ionic leak currents, and I_D^{Int} and I_S^{Int} are the intrinsic currents for the dendritic and axosomatic compartments respectively. The intrinsic currents for the dendritic and axosomatic compartments have been previously described in (Krishnan and Bazhenov, 2011; González et al., 2015; Krishnan et al., 2015).

2.6. Dynamic ion concentrations

Ionic concentrations dynamics for $[K^+]_o$, $[K^+]_i$, $[Na^+]_o$, $[Na^+]_i$, $[Ca^{2+}]_i$, and $[Cl^-]_i$ were modeled similar to our previous work (Krishnan and Bazhenov, 2011; González et al., 2015;

Krishnan et al., 2015). In order to model the KCC2 co-transporter, we made some modifications to the $[K^+]_o$ and $[Cl^-]_i$ equations. Briefly, our previous models included KCC2 regulation of $[Cl^-]_i$ in a $[K^+]_o$ dependent manner. However, the $[K^+]_o$ was not affected by KCC2 activity. In this new study the $[K^+]_o$ and $[Cl^-]_i$ were modeled as follows:

$$\frac{d[K^+]_o}{dt} = \left(\frac{k}{Fd}\right)(I_K^{pump} + I_{\sum K}^{Int} + I_{KCC2}) + \delta_o([K^+]_{oc} - [K^+]_o) + G$$
$$+ \delta_o\left(\left(\frac{([K^+]_{o-1} + [K^+]_{o+1})}{2} + \gamma([K^+]_{ox})\right)/(1+\gamma) - [K^+]_o\right)$$
$$\frac{d[Cl^-]_i}{dt} = -\left(\frac{k}{F}\right)(I_{\sum Cl}^{Int} + I_{KCC2})$$

where $F = 96489$ C/mol is the Faraday constant, the ratio of the extracellular volume to surface area is given by $d = 0.15$, and the conversion factor $k = 10$. Additionally, I_K^{pump} is the K^+ current through the Na$^+$/K$^+$ ATPase, $[K^+]_{oc}$ is the K^+ concentration in the adjacent compartment, $[K^+]_{o-1}$ and $[K^+]_{o+1}$ are the concentrations of K^+ neighboring cells. $\gamma = 0.06$ is the ion coupling coefficient between PNs and INs, $[K^+]_{ox}$ is the K^+ concentration of the neighboring IN when computing the $[K^+]_o$ for PNs and vice versa. δ_o is the scaled diffusion coefficient ($\delta_o = D/x$), where $D = 6\times10^{-6}$ cm^2/s is the diffusion constant, $x = 100$ μm is distance, and G represents the glial buffering of K^+ as described in detail previously (Krishnan and Bazhenov, 2011; González et al., 2015; Krishnan et al., 2015). $I_{\sum K}^{Int}$ and $I_{\sum Cl}^{Int}$ are the sum total intrinsic K^+ and Cl^- currents respectively. I_{KCC2} defines the efflux of $[K^+]_o$ and $[Cl^-]_i$ generated by the KCC2 co-transporter and is described as follows:

$$I_{KCC2} = \left(\frac{\alpha_{KCC2}}{1+\exp(([Cl^-]_{i\infty} - [Cl^-]_i)/1.0)}\right)\left(\frac{[Cl^-]_{i\infty} - [Cl^-]_i}{\tau_{Cl}}\right)$$
$$\tau_{Cl} = \left(100 + \frac{\tau_{Cl\infty}}{\left(1+\exp\left(\frac{[Cl^-]_{i\infty} - [K^+]_o}{\tau_{KoCl}}\right)\right)}\right)$$

where $a_{KCC2} = 80$ defines the strength of the co-transporter, $[Cl^-]_{i\infty} = 5$mM is the steady-state Cl^- concentration, $[Cl^-]_i$ is the intracellular Cl^- concentration, $\tau_{Cl\infty} = 4\times10^3$s, and $\tau_{KoCl} = 0.08$s.

2.7. Synapse and network properties

We modeled a one dimensional network consisting of 100 PNs and 20 INs. Every PN formed local excitatory synapses onto ten neighboring PNs with AMPA conductance strength of 3.5 nS and NMDA conductance of 0.9 nS. PNs also formed excitatory synaptic connections onto INs with AMPA and NMDA conductance strengths of 2.4 nS and 0.24 nS respectively. INs synapsed onto five local PNs, with GABA$_A$ connections of 3.5 nS conductance strength. Additionally, PN and IN received individual afferent excitatory input

modeled as a Poisson process as described in our previous studies (Krishnan and Bazhenov, 2011; González et al., 2015; Krishnan et al., 2015).

2.8. Estimation of seizure threshold

The seizure threshold was determined using a binary search method that employed an iterative procedure as described in (González et al., 2015). Briefly, at each step of the searching algorithm, the strength of the stimulus would be set to the mean of the upper and lower limits, <*P*>. If this stimulus strength was able to elicit seizure, the upper limit would be set to the current value of <*P*>. If <*P*> was unable to elicit a seizure, the lower limit would take the value of <*P*>. The new stimulus strength, <*P*>, would then be computed based on the updated upper and lower limits. This process continued until the difference between the upper and lower limits was less than 0.1. The threshold was determined to be the average of these final limits.

3. Results

3.1. Optogenetic stimulation of interneurons triggers ictal discharges

Spontaneous 4AP-induced ictal discharges were recorded from the entorhinal cortex (EC) of PV-Cre mice that were transcranially injected with the enhanced ChR2 opsin, ChETA (n = 5 slices). These discharges occurred every 158.07 ± 10.30 s with an average duration of 45.97 ± 1.33 s (n = 124 events). Using a 30 s train of 1 s light pulses at 0.2 Hz that optogenetically activated fast-spiking parvalbumin (PV)-positive interneurons, we were able to trigger ictal discharges of similar duration (i.e., 43.91 ± 2.27 s) but more frequently, at an average interval of 139.45 ± 4.79 s (n = 35 events; $p < 0.05$; ure 1A).

Next, we established whether the ability of interneuron activation to drive ictal discharges was linked exclusively to fast-spiking PV-positive interneurons, or whether ictal discharges could also be triggered by activating regular-spiking somatostatin (SOM)-positive interneurons. Therefore, we obtained brain slices containing the EC of SOM-Cre mice that had been transcranially injected with the ChETA opsin (n = 8 slices). Spontaneous 4AP-induced ictal discharges in these experiments occurred every 127.35 ± 6.30 s and lasted on average 63.28 ± 1.84 s (n = 126 events). Using the same protocol used to stimulate PV-interneurons (i.e. 1 s light pulses at 0.2 Hz for 30 s), we were able to trigger ictal discharge of similar duration (55.71 ± 1.90 s), but at a shorter interval of 104.56 ± 5.47 s (n = 44 events; $p < 0.05$; figure 1B). The ictal discharges elicited by the optogenetic activation of either PV- or SOM-expressing interneurons showed characteristic properties of low-voltage, fast (LVF) ictal discharges. Previously, we showed that these LVF ictal discharges are different from the hypersynchronous (HYP) ictal discharges induced by optogenetic stimulation of CamKII-positive principal neurons suggesting a different mechanism between principal neuron- and inhibitory interneuron-induced ictal discharges (Shiri et al., 2016).

3.2. Reduction of I_A primes the network for interneuron-induced seizure-like activity

In order to establish the mechanisms by which PV- and SOM-interneuron stimulation causes ictal discharges in brain slices treated with 4AP, we developed a biophysically realistic network model implementing dynamic ion concentrations, the electrogenic Na^+/K^+ pump,

and the KCC2 co-transporter. The network contained synaptically coupled principal (excitatory) neurons (PN) and inhibitory interneurons (IN), where the extracellular compartments of these two neuron types were ionically coupled (see Methods). In order to make comparisons between our model and experimental data, we modeled the application of 4AP as resulting in a 50 percent reduction of the outward K^+ A-current. Additionally, optogenetic stimulation of interneurons was modeled as a series of 1 s pulses at 0.2 Hz for 30 s similar to those used in our *in vitro* experiments; these "activating" pulses were applied to all interneurons.

In a control network, one without reduction of I_A, the stimuli applied to INs resulted in increased firing rate for the duration of the stimulation, followed by a gradual decay back to baseline firing (figure 2A). During baseline activity, the mean IN firing rate fluctuated around 1 Hz, but during stimulation it reached ~25 Hz (figure 2C, red). The increase in IN firing during stimulus pulses was accompanied by a hyperpolarization and relative silencing of the postsynaptic PNs (figure 2B and C, black trace). Similar to INs, PNs displayed a gradual return to a baseline mean firing rate of about 5 Hz (figure 2C, black trace). This control network behaved as expected, i.e., the transient increase in IN firing caused a transient hyperpolarization of the PNs followed by a gradual return to the baseline activity.

We next tested the effects induced by IN stimulation on the network dynamics during conditions mimicking 4AP application, i.e., a reduction of I_A in both PNs and INs that resulted in a slight increase of the mean intrinsic baseline firing rates of both cell types (~ 4 Hz and ~ 12 Hz for INs and PNs respectively; figure 3D). In this condition, a single stimulus applied to INs produced an expected hyperpolarization and silencing of PN activity. We then proceeded to apply a sequence of the stimuli to all INs to model the effect of optogenetic stimulation similar to our experiment in the control network (figure 2). IN firing peaked at ~ 35 Hz during each stimulus pulse (figure 3A and D, red trace), and during the first 2 pulses PNs were hyperpolarized and silenced by the IN-mediated inhibition (figure 3B and C). However, during subsequent stimulation pulses, the mean firing rate of PNs began to increase (figure 3D, black trace), and the network developed a seizure-like state, which initiated as focal tonic firing (figure 3B, cells 60–100) before spreading to the rest of the network, and eventually transitioning to a clonic bursting phase (figure 3B and C). Seizure termination was followed by the postictal depression, and then by a return to baseline firing in both neuron types.

Since reduction of I_A shifted the network to a state where synchronous inhibitory activity could induce seizure, we next tested the effect of I_A strength on the seizure threshold. Reduction of I_A made networks more susceptible to seizure (figure 3E; 40–60% range), which can be attributed to increased intrinsic network excitability due to reduced K^+-dependent inhibition. I_A strengths less than 40% of the baseline resulted in spontaneous seizures, while strengths greater than 60% did not allow transitions to seizure-like activity following interneuron stimulation.

Dynamics of the $[K^+]_o$ and $[Cl^-]_i$ under these two network conditions – i.e., control and under reduced I_A (figures 2 and 3) - revealed stark differences following IN stimulation. As seen in figure 4A, mean $[Cl^-]_i$ and $[K^+]_o$ for all PNs behaved similarly prior to and during

IN stimulation in both control and reduced I_A networks (red and black traces respectively). During IN stimulation, both networks revealed increases in the mean $[Cl^-]_i$, and initial decreases in $[K^+]_o$ (figure 4A). The increase in $[Cl^-]_i$ in PNs was presumably due to activation of postsynaptic $GABA_A$ receptors, while the transient (initial) decrease in $[K^+]_o$ could reflect the resulting reduction of PN firing. Following termination of the IN stimulation, the $[Cl^-]_i$ in the control network gradually returned to baseline along with the IN firing rate (figure 2C, red trace and figure 4A, red trace in left panel). PN firing became transiently elevated but then also returned to baseline (Fig. 2C, black trace). In contrast, under conditions of I_A reduction, IN firing remained elevated and $[Cl^-]_i$ continued to increase following the end of the stimulation (figure 2C, red trace and figure 4A, black trace in left panel). Accumulation of $[Cl]_i$ caused activation of the KCC2 co-transporter. As KCC2 uses K^+ gradient to remove Cl^- (Payne et al., 2003), activation of KCC2 led to accumulation of $[K^+]_o$ (figure 4A, right panel, black trace). This increased PNs excitability (already elevated under reduced I_A conditions) and triggered a positive feedback loop (Frohlich and Bazhenov, 2006; Frohlich et al., 2008; Krishnan and Bazhenov, 2011) initiating a network transition to seizure-like activity (figure 4B and 4C). It is important to emphasize, that while the increase of $[Cl^-]_i$ reduced the effect of inhibition, Cl^- reversal potential never raised above the resting membrane potential of PNs and, therefore, the effect of $GABA_A$ remained hyperpolarizing throughout the entire simulation time.

Both $[Cl^-]_i$ in PNs and $[K^+]_o$ in the surrounding extracellular space remained elevated during the seizure-like activity (figure 4B and C, respectively). The expanded sample shown in figure 4D illustrates how activation of INs resulted in the silencing and hyperpolarization of PNs during stimulation pulses, while the subsequent accumulation of $[K^+]_o$ increased firing rate and eventually triggered the transition to seizure-like activity. These results reveal that in conditions of increased baseline excitability (such as after reducing I_A), the network is able to generate seizure-like activity following interneuron activation. Our model suggests that the mechanism of seizure initiation involves: (a) IN stimulation leading to the release of GABA and postsynaptic activation of $GABA_A$ receptors; (b) $GABA_A$ receptor activation leading to increase of $[Cl^-]_i$ mediating KCC2 activation; (c) KCC2 activation leading to increase of $[K^+]_o$ sufficiently to initiate the positive feedback loop that mediates an "avalanche" increase of excitability.

3.3. KCC2 co-transporter activity gives rise to interneuron-induced seizure-like activity

To directly test our hypothesis that an increase of KCC2 activity, resulting from $[Cl^-]_i$ accumulation, may underlie initiation of seizure-like activity, we reduced KCC2 co-transporter strength by 50 percent ($a_{KCC2}= 40$, see Methods) in a network with reduced I_A, while stimulating INs (figure 5). IN stimulation was identical to that performed in the previous experiments (figures 2 and 3). In this new condition, stimulation of INs resulted only in the transient silencing of PN activity (figure 5A, top), and $[K^+]_o$ returned to the baseline levels shortly after the termination of IN stimulation (figure 5A, bottom). Unlike the results shown in figure 3, no transition to seizure-like activity occurred during or following the termination of IN stimulation. Note, however, that the reduction of KCC2 activity resulted in a less excitable network, which was caused by a decrease of $[K^+]_o$ accumulation due to the reduced KCC2 baseline activity.

To further demonstrate that accumulation of $[Cl^-]_i$ was directly responsible for the activation of the KCC2 co-transporter and subsequent accumulation of $[K^+]_o$, in the next experiment we reduced the effect of KCC2 on the ion concentrations, but prevented the reduction of baseline network activity (Fig. 5A). Thus, we kept the strength of KCC2 intact (a_{KCC2} = 80), but we capped the maximal amount of Cl^- that can enter both PNs and INs. In doing so, we limited the peak KCC2 activity without changing the baseline KCC2 activity and, therefore, baseline network firing rate. In this condition, IN stimulation was still unable to initiate a seizure-like response (figure 5B). $[Cl^-]_i$ increased during IN stimulation, however, it was unable to induce sufficient activation of the KCC2 co-transporter to trigger high $[K^+]_o$ increase. Thus, following IN stimulation, only a small and brief increase in $[K^+]_o$ was observed (figure 5B, bottom). This suggests that limiting KCC2 performance may prevent transition to the seizure-like activity. We need to mention, however, that limiting peak $[Cl^-]_i$ level also affected other network properties (e.g., reversal potential of Cl^- and therefore effect of inhibition).

Since limiting $[Cl^-]_i$ increase could affect several properties of the model, in the next experiment we artificially limited the effect of $[Cl^-]_i$ on the KCC2 co-transporter only. Therefore, in this condition, though the $[Cl^-]_i$ could exhibit a significant increase, the KCC2 co-transporter would only sense a limited increase in $[Cl^-]_i$. That is, the value of the variable in the I_{KCC2} equation representing intracellular Cl^- concentration (see Methods) was kept below the actual amount of $[Cl^-]_i$. Essentially, this rendered the K^+ extrusion mechanism of the KCC2 co-transporter less sensitive to $[Cl^-]_i$. As shown in figure 5C, IN stimulation was unable to elicit seizure-like activity in this network. Brief increases in both $[Cl^-]_i$ and $[K^+]_o$ were observed following the stimulation (figure 5C, bottom). Though the KCC2 activity increased $[K^+]_o$ following IN stimulation, $[K^+]_o$ never reached concentrations sufficient for generation of seizure-like activity. Importantly $[Cl^-]_i$ could reach its peak level (the same as in control model) in this experiment, suggesting that the shift of the $GABA_A$ reversal potential, associated with increase of $[Cl^-]_i$, alone is not sufficient to induce seizure-like activity.

Finally, we tested whether a direct increase in $[Cl^-]_i$ in PNs could lead to the activation of the KCC2 co-transporter and subsequent elevation of $[K^+]_o$. In this experiment, we used a baseline model where the effect of $[Cl^-]_i$ on KCC2 was intact (similar to network in figure 3). We found that a brief and sufficiently strong increase of $[Cl^-]_i$ in PNs was able to activate KCC2 extrusion of K^+ followed by the development of seizure-like activity (figure 5D). Together, these data suggest that Cl^- specific activation of KCC2 activity gives rise to the increase in $[K^+]_o$ sufficient for triggering transition to seizure-like activity.

3.4. $GABA_A$, and KCC2 influence properties of interneuron-induced seizure-like activity

Our model predicts that $GABA_A$ receptor-dependent increase in $[Cl^-]_i$ results in KCC2 mediated increase of $[K^+]_o$ and may lead to the initiation of seizure. Next, we tested how these two specific properties affect seizure onset and duration. By changing contribution of $GABA_A$ to the $[Cl^-]_i$ in the model, we found that limiting $[Cl^-]_i$ increase in PNs increased the seizure threshold (figure 6A). Reducing $GABA_A$ receptor-dependent increase of $[Cl^-]_i$ to 94 % of the baseline, prevented IN stimulation from inducing seizure-like activity in the

model. The reduced contribution of $GABA_A$ receptor activations to the $[Cl^-]_i$ also resulted in the shorter seizure duration (figure 6C). Both these effects arise from the fact that reduced $[Cl^-]_i$ accumulation led to the lower KCC2 activation and reduced K^+ efflux.

This prediction was further validated by directly changing KCC2 strength (a_{KCC2}). As illustrated in figure 6B, increasing KCC2 strength decreased seizure threshold, while decreasing KCC2 strength led to the threshold increase. Decreasing KCC2 strength also resulted in a decrease of seizure duration, while increased KCC2 strength had an opposite effect (figure 6D and F). Interestingly, reduction of KCC2 strength also delayed the onset time of seizure-like activity (figure 6E). Between the network with control (100 %) KCC2 activity and the network with low KCC2 activity (figure 6F, blue), there was a difference of about 11 sec for the seizure onset time. In the networks with stronger KCC2 (figure 6E, green), seizure onset occurred earlier as compared to that in a control network with 100% KCC2 strength. This effect can be explained by the different rate of $[K^+]_o$ accumulation resulting from KCC2 activity. When KCC2 activity was enhanced, $[K^+]_o$ accumulated faster and reached the critical threshold that was sufficient for initiation of seizure-like activity after only a few seconds.

4. Discussion

Application of potassium channel blocker 4AP may lead to epileptiform activity both *in vivo* and *in vitro* (Avoli and de Curtis, 2011). Optogenetic activation of inhibitory interneurons, in acute mouse brain slices exposed to 4AP, triggered seizure-like discharges (Sessolo et al., 2015; Yekhlef et al., 2015; Shiri et al., 2016). Blocking KCC2 activity with either VU024055 or high doses of bumetanide abolished ictal discharges in 4AP-treated rat brain slices (Hamidi and Avoli, 2015), suggesting that this form of inhibition-induced seizure may involve activation of the KCC2 co-transporter. In this new study, we tested the hypothesis that in conditions of elevated cortical excitability (as in the presence of 4AP), Cl^--dependent activation of the KCC2 co-transporter can trigger the progression of a network to a seizure state by an increase of extracellular K^+. Our *in vitro* data and computer simulation results predict that synchronous activation of the inhibitory interneurons can lead to a Cl^- increase sufficient for KCC2 activation and development of paroxysmal activity. This mechanism does not require synaptic $GABA_A$ to inverse polarity as the epileptiform activity is mediated by increase of the extracellular K^+ and not by the depolarizing effect of the $GABA_A$ signaling, which remains inhibitory.

4.1. K^+ channelopathies in epilepsy

Various channelopathies, including mutated or misregulated K^+ channels, have been suggested to underlie certain forms of genetic epilepsies (D'Adamo et al., 2013; Lascano et al., 2016). Indeed, mutations in K_V4 α-subunits are present in some patients suffering from pharmacoresistant temporal lobe epilepsy (Singh et al., 2006; D'Adamo et al., 2013). Specifically, a truncation mutation of the $K_V4.2$ α-subunit, responsible for the I_A, was observed in human patients (Singh et al., 2006). This mutation results in an attenuated I_A and subsequent increases in seizure susceptibility. In addition to mutations of specific ion channels, mutations of genes encoding proteins which modulate ion channel activity were

found. Patients suffering from autosomal dominant partial epilepsy with auditory features (ADPEAF) have been shown to have point mutations in the leucine-rich glioma-inactivated 1 (LGI1) gene, resulting in reduced neuronal secretion of LGI1 (Ottman et al., 2004; Nobile et al., 2009; Dazzo et al., 2015). Neuronally secreted LGI1 binds to $K_V1.4$ and $K_V\beta1$, two known subunits comprising the A-type channels, preventing rapid inactivation of A-type currents (Schulte et al., 2006). The reduction of LGI1 expression in patients with ADPEAF results in the rapid inactivation of A-type channels and subsequent hyperexcitability.

The I_A antagonist, 4AP, has been shown to cause increased neuronal excitability and seizure-like discharges *in vivo* (Fragoso-Veloz et al., 1990; Levesque et al., 2013) and *in vitro* (Avoli et al., 1996; Lopantsev and Avoli, 1998). Interestingly, direct knockout of the $K_V4.2$ α-subunit resulted in increased excitability but did not generate spontaneous seizures. This knockout can, however, increase seizure susceptibility in response to additional proconvulsive pharmacological agents (Barnwell et al., 2009). Previous studies proposed that reduction of A-type K^+ current promotes ictogenesis by directly increasing neuronal excitability (Galvan et al., 1982; Gustafsson et al., 1982; Yamaguchi and Rogawski, 1992). In contrast, our study predicts that the reduction of A-type K^+ current leads to increased excitability of both excitatory and inhibitory neurons, and that the latter is critical for epileptogenesis. We show that acute brain slices treated with 4AP exhibit transitions to seizure when perturbed by photostimulation of inhibitory interneurons. Using computer modeling, we tested the hypothesis that the mechanism by which increased GABAergic signaling may lead to paroxysmal discharges involves Cl^--dependent activation of KCC2 followed by increases in the extracellular K^+.

4.2. GABA_A receptor-dependent $[K^+]_o$ excitatory transients

Early studies proposed that reduced inhibition underlies seizure generation and perhaps epilepsy (Ben-Ari et al., 1979; Dingledine and Gjerstad, 1980; Schwartzkroin and Prince, 1980). Later, this view was challenged in several studies, (de Curtis and Avoli, 2016), which revealed that synchronous inhibitory interneuron activity occurs prior to seizure onset in slices treated with 4AP (Lillis et al., 2012; Uva et al., 2015; Levesque et al., 2016). It has been reported that intense GABAergic stimulation results in an increase of $[K^+]_o$ and long-lasting depolarizations (Rivera et al., 2005; Viitanen et al., 2010). Additionally, application of either bicuculline or furosemide inhibits these events (Viitanen et al., 2010). Indeed, these GABAergic excitatory $[K^+]_o$ transients have been shown to elicit prolonged depolarizations in rat CA1 and EC, and may play a prominent role in seizure generation (Lopantsev and Avoli, 1998; Viitanen et al., 2010). The proconvulsive GABAergic excitatory $[K^+]_o$ transients may give rise to the spontaneous seizure onset in patients with K^+ channel abnormalities.

In vitro and *in silico* results presented in this study predict the mechanisms by which GABAergic signaling can trigger seizure onset. We propose that the increased GABAergic signaling, such as triggered by stimulation of inhibitory interneurons, induces Cl^- build up, followed by Cl^- dependent activation of the KCC2 co-transporter and subsequent increase of $[K^+]_o$. Indeed, high frequency stimulation has been shown to cause increases in $[K^+]_o$ in response to intense $GABA_A$ receptor activation (Ruusuvuori et al., 2004; Rivera et al., 2005;

Viitanen et al., 2010). Optogenetic stimulation of either SOM- or PV-expressing interneurons also causes large increases in $[K^+]_o$ (Yekhlef et al., 2015). It has been shown that sufficiently large initial increase of $[K^+]_o$ can give rise to a positive feedback loop due to an increase in the network excitability through $[K^+]_o$ dependent depolarization of neurons, which in turn results in a further increase of $[K^+]_o$ and can lead to epileptiform activity (Somjen, 2002; Frohlich and Bazhenov, 2006; Frohlich et al., 2008; Krishnan and Bazhenov, 2011; Wei et al., 2014; González et al., 2015; Krishnan et al., 2015). Our new study predicts that the mechanisms leading to the initial increase in $[K^+]_o$, which kicks the network into a vicious feedback cycle, may involve KCC2-dependent efflux of K^+.

4.3. KCC2 in epilepsy

It has been shown that during early stages of development, GABAergic signaling in the rodent brain produces depolarizing potentials (Payne et al., 2003; Ben-Ari et al., 2007). The transition from depolarizing to hyperpolarizing GABAergic signaling has been attributed to the changes in Cl^- homeostasis as the animal develops (Payne et al., 2003; Watanabe and Fukuda, 2015). During early stages of development, the Na^+-K^+-Cl^- co-transporter (NKCC1) - responsible for transporting two Cl^- ions and one K^+ and Na^+ ion into the neuron - is highly expressed in rat and mouse neurons (Dzhala et al., 2005). As a result $[Cl^-]_i$ can reach baseline concentrations of 30mM (Achilles et al., 2007) resulting in depolarization of the Cl^- reversal potential, and making GABAergic signaling depolarizing. As the brain develops, NKCC1 expression levels decrease, and KCC2 expression increases (Watanabe and Fukuda, 2015). Indeed, KCC2 mRNA is not detected until E18.5 and E15.5 in mouse CA1 and CA3 hippocampal subfields, respectively, while by P15, KCC2 and NKCC1 expression in the mouse brain reaches adult levels (Watanabe and Fukuda, 2015). In our current study, as well as in previous reports (Sessolo et al., 2015; Yekhlef et al., 2015; Shiri et al., 2016), epileptiform activity was induced through optogenetic stimulation of inhibitory interneurons in juvenile and young adult mice ranging from P15 to P40 during 4AP treatment. Furthermore, experiments in adult rats have shown that the KCC2 co-transporter plays a prominent role in the development of 4AP-induced epileptiform activity (Avoli et al., 1996; Lopantsev and Avoli, 1998; Hamidi and Avoli, 2015). Together, these results suggest that the "epileptogenic" effect of interneuron activation in 4AP conditions, as described in our study, does not depend on the reversal of the $GABA_A$ synaptic potential as found early in development, but may rely on the mechanisms that were tested in our computational model. These mechanisms rest on the increase in the extracellular K^+ concentrations that result from KCC2 activation, triggered by an increase of intracellular Cl^- during intense interneuron firing.

Downregulation of KCC2 expression levels have been suggested to underlie the development of epilepsy in patients (Huberfeld et al., 2007; Buchin et al., 2016). However, other studies have shown that increased KCC2 activation may play a prominent role in seizure generation (Viitanen et al., 2010; Hamidi and Avoli, 2015). Activity dependent regulation of KCC2 expression may explain this seemingly conflicting evidence. Indeed, KCC2 expression has been shown to reduce following increases in activity and epileptiform discharges (Rivera et al., 2002; Rivera et al., 2004; Rivera et al., 2005). Our computational model revealed that the reduction of KCC2 activity prevents seizures in response to intense

GABAergic signaling, suggesting that the observed reduction of KCC2 expression may not be a seizure triggering factor, but rather a protective mechanism to reduce the likelihood of seizures being triggered by other factors. Our study predicts that an increase of $[Cl^-]_i$ in excitatory neurons activates KCC2 co-transporter and promotes initiation of seizure. Consistent with this prediction, recent experimental studies reported large increase in $[Cl^-]_i$ in excitatory neurons prior to paroxysmal discharges (Lillis et al., 2012). Our model also predicts that increases in KCC2 activity can increase seizure susceptibility and duration. This result is consistent with previous computational modelling and experimental work (Krishnan and Bazhenov, 2011; Hamidi and Avoli, 2015). Importantly, our model predicts a complex effect of $GABA_A$ inhibition in seizure development. On one hand, increase of $GABA_A$ signaling would act to suppress the network activity, on the other it would promote increase of $[Cl^-]_i$ in excitatory neurons which drives KCC2 activation and $[K^+]_o$ efflux, thus paradoxically increasing network excitability. The balance of these opposite factors determines the resulting network dynamics (normal vs epileptic) in the physiological settings.

5. Conclusions

Patients suffering from pharmacoresistant seizures make up approximately 30% of the total number of people living with epilepsy (Nadkarni et al., 2005; Perucca and Tomson, 2011). Among the commonly prescribed antiepileptic drugs, several of them (such as benzodiazepine and barbiturates) enhance $GABA_A$ receptor function (Nadkarni et al., 2005; Perucca and Tomson, 2011). Our new study suggests that increased GABAergic signaling, through treatment with these antiepileptic drugs, may exacerbate existing seizures in patients with K^+ channelopathies. We predict that modulation of KCC2 activity may prevent seizure generation in patients. Thus, our findings may provide a new avenue for pharmacological interventions in patients suffering from intractable epilepsy due to K^+ channelopathies.

Acknowledgments

References

Avoli M, Barbarosie M, Lücke A, Nagao T, Lopantsev V, Köhling R. Synchronous GABA-mediated potentials and epileptiform discharges in the rat limbic system in vitro. J Neurosci. 1996; 16:3912–3924. [PubMed: 8656285]

Achilles K, Okabe A, Ikeda M, Shimizu-Okabe C, Yamada J, Fukuda A, Luhmann HJ, Kilb W. Kinetic properties of Cl uptake mediated by Na+-dependent K+-2Cl cotransport in immature rat neocortical neurons. J Neurosci. 2007; 27:8616–8627. [PubMed: 17687039]

Avoli M, de Curtis M. GABAergic synchronization in the limbic system and its role in the generation of epileptiform activity. Prog Neurobiol. 2011; 95:104–132. [PubMed: 21802488]

Avoli M, Barbarosie M, Lucke A, Nagao T, Lopantsev V, Kohling R. Synchronous GABA-mediated potentials and epileptiform discharges in the rat limbic system in vitro. J Neurosci. 1996; 16:3912–3924. [PubMed: 8656285]

Avoli M, de Curtis M, Gnatkovsky V, Gotman J, Kohling R, Levesque M, Manseau F, Shiri Z, Williams S. Specific imbalance of excitatory/inhibitory signaling establishes seizure onset pattern in temporal lobe epilepsy. J Neurophysiol. 2016; 115:3229–3237. [PubMed: 27075542]

Barnwell LF, Lugo JN, Lee WL, Willis SE, Gertz SJ, Hrachovy RA, Anderson AE. Kv4.2 knockout mice demonstrate increased susceptibility to convulsant stimulation. Epilepsia. 2009; 50:1741–1751. [PubMed: 19453702]

Bazhenov M, Timofeev I, Steriade M, Sejnowski TJ. Model of thalamocortical slow-wave sleep oscillations and transitions to activated States. J Neurosci. 2002; 22:8691–8704. [PubMed: 12351744]

Bazhenov M, Timofeev I, Steriade M, Sejnowski TJ. Potassium model for slow (2–3 Hz) in vivo neocortical paroxysmal oscillations. J Neurophysiol. 2004; 92:1116–1132. [PubMed: 15056684]

Ben-Ari Y, Krnjevi K, Reinhardt W. Hippocampal seizures and failure of inhibition. Canadian Journal of Physiology and Pharmacology. 1979; 57:1462–1466.

Ben-Ari Y, Gaiarsa JL, Tyzio R, Khazipov R. GABA: a pioneer transmitter that excites immature neurons and generates primitive oscillations. Physiol Rev. 2007; 87:1215–1284. [PubMed: 17928584]

Buchin A, Chizhov A, Huberfeld G, Miles R, Gutkin BS. Reduced Efficacy of the KCC2 Cotransporter Promotes Epileptic Oscillations in a Subiculum Network Model. J Neurosci. 2016; 36:11619–11633. [PubMed: 27852771]

D'Adamo MC, Catacuzzeno L, Di Giovanni G, Franciolini F, Pessia M. K(+) channelepsy: progress in the neurobiology of potassium channels and epilepsy. Front Cell Neurosci. 2013; 7:134. [PubMed: 24062639]

Dazzo E, Santulli L, Posar A, Fattouch J, Conti S, Loden-van Straaten M, Mijalkovic J, De Bortoli M, Rosa M, Millino C, Pacchioni B, Di Bonaventura C, Giallonardo AT, Striano S, Striano P, Parmeggiani A, Nobile C. Autosomal dominant lateral temporal epilepsy (ADLTE): novel structural and single-nucleotide LGI1 mutations in families with predominant visual auras. Epilepsy Res. 2015; 110:132–138. [PubMed: 25616465]

de Curtis M, Avoli M. GABAergic networks jump-start focal seizures. Epilepsia. 2016; 57:679–687. [PubMed: 27061793]

Dingledine R, Gjerstad L. Reduced inhibition during epileptiform activity in the in vitro hippocampal slice. J Physiol. 1980; 305:297–313. [PubMed: 7441555]

Dzhala VI, Talos DM, Sdrulla DA, Brumback AC, Mathews GC, Benke TA, Delpire E, Jensen FE, Staley KJ. NKCC1 transporter facilitates seizures in the developing brain. Nat Med. 2005; 11:1205–1213. [PubMed: 16227993]

Fragoso-Veloz J, Massieu L, Alvarado R, Tapia R. Seizures and wet-dog shakes induced by 4-aminopyridine, and their potentiation by nifedipine. Eur J Pharmacol. 1990; 178:275–284. [PubMed: 2340861]

Frohlich F, Bazhenov M. Coexistence of tonic firing and bursting in cortical neurons. Phys Rev E Stat Nonlin Soft Matter Phys. 2006; 74:031922. [PubMed: 17025682]

Frohlich F, Bazhenov M, Iragui-Madoz V, Sejnowski TJ. Potassium dynamics in the epileptic cortex: new insights on an old topic. Neuroscientist. 2008; 14:422–433. [PubMed: 18997121]

Galvan M, Grafe P, ten Bruggencate G. Convulsant actions of 4-aminopyridine on the guinea-pig olfactory cortex slice. Brain Res. 1982; 241:75–86. [PubMed: 7104708]

González OC, Krishnan GP, Chauvette S, Timofeev I, Sejnowski T, Bazhenov M. Modeling of Age-Dependent Epileptogenesis by Differential Homeostatic Synaptic Scaling. The Journal of Neuroscience. 2015; 35:13448–13462. [PubMed: 26424890]

Grasse DW, Karunakaran S, Moxon KA. Neuronal synchrony and the transition to spontaneous seizures. Experimental neurology. 2013; 248:72–84. [PubMed: 23707218]

Gustafsson B, Galvan M, Grafe P, Wigstrom H. A transient outward current in a mammalian central neurone blocked by 4-aminopyridine. Nature. 1982; 299:252–254. [PubMed: 6287290]

Hamidi S, Avoli M. KCC2 function modulates in vitro ictogenesis. Neurobiol Dis. 2015; 79:51–58. [PubMed: 25926348]

Houweling AR, Bazhenov M, Timofeev I, Steriade M, Sejnowski TJ. Homeostatic synaptic plasticity can explain post-traumatic epileptogenesis in chronically isolated neocortex. Cereb Cortex. 2005; 15:834–845. [PubMed: 15483049]

Huberfeld G, Wittner L, Clemenceau S, Baulac M, Kaila K, Miles R, Rivera C. Perturbed chloride homeostasis and GABAergic signaling in human temporal lobe epilepsy. J Neurosci. 2007; 27:9866–9873. [PubMed: 17855601]

Krishnan GP, Bazhenov M. Ionic dynamics mediate spontaneous termination of seizures and postictal depression state. J Neurosci. 2011; 31:8870–8882. [PubMed: 21677171]

Krishnan GP, Filatov G, Shilnikov A, Bazhenov M. Electrogenic properties of the Na(+)/K(+) ATPase control transitions between normal and pathological brain states. J Neurophysiol. 2015; 113:3356–3374. [PubMed: 25589588]

Lascano AM, Korff CM, Picard F. Seizures and Epilepsies due to Channelopathies and Neurotransmitter Receptor Dysfunction: A Parallel between Genetic and Immune Aspects. Mol Syndromol. 2016; 7:197–209. [PubMed: 27781030]

Levesque M, Salami P, Behr C, Avoli M. Temporal lobe epileptiform activity following systemic administration of 4-aminopyridine in rats. Epilepsia. 2013; 54:596–604. [PubMed: 23521339]

Levesque M, Herrington R, Hamidi S, Avoli M. Interneurons spark seizure-like activity in the entorhinal cortex. Neurobiol Dis. 2016; 87:91–101. [PubMed: 26721318]

Librizzi L, Losi G, Marcon I, Sessolo M, Scalmani P, Carmignoto G, de Curtis M. Interneuronal network activity at the onset of seizure-like events in entorhinal cortex slices. The Journal of Neuroscience. 2017

Lillis KP, Kramer MA, Mertz J, Staley KJ, White JA. Pyramidal cells accumulate chloride at seizure onset. Neurobiol Dis. 2012; 47:358–366. [PubMed: 22677032]

Lopantsev V, Avoli M. Participation of GABAA-mediated inhibition in ictallike discharges in the rat entorhinal cortex. J Neurophysiol. 1998; 79:352–360. [PubMed: 9425204]

Nadkarni S, LaJoie J, Devinsky O. Current treatments of epilepsy. Neurology. 2005; 64:S2–11. [PubMed: 15994220]

Nobile C, Michelucci R, Andreazza S, Pasini E, Tosatto SC, Striano P. LGI1 mutations in autosomal dominant and sporadic lateral temporal epilepsy. Hum Mutat. 2009; 30:530–536. [PubMed: 19191227]

Ottman R, Winawer MR, Kalachikov S, Barker-Cummings C, Gilliam TC, Pedley TA, Hauser WA. LGI1 mutations in autosomal dominant partial epilepsy with auditory features. Neurology. 2004; 62:1120–1126. [PubMed: 15079011]

Payne JA, Rivera C, Voipio J, Kaila K. Cation-chloride co-transporters in neuronal communication, development and trauma. Trends Neurosci. 2003; 26:199–206. [PubMed: 12689771]

Pedley TA, Fisher RS, Moody WJ, Futamachi KJ, Prince DA. Extracellular potassium activity during epileptogenesis: a comparison between neocortex and hippocampus. Trans Am Neurol Assoc. 1974; 99:41–45. [PubMed: 4463561]

Perucca E, Tomson T. The pharmacological treatment of epilepsy in adults. Lancet Neurol. 2011; 10:446–456. [PubMed: 21511198]

Rivera C, Voipio J, Kaila K. Two developmental switches in GABAergic signalling: the K+-Cl-cotransporter KCC2 and carbonic anhydrase CAVII. J Physiol. 2005; 562:27–36. [PubMed: 15528236]

Rivera C, Voipio J, Thomas-Crusells J, Li H, Emri Z, Sipila S, Payne JA, Minichiello L, Saarma M, Kaila K. Mechanism of activity-dependent downregulation of the neuron-specific K-Cl cotransporter KCC2. J Neurosci. 2004; 24:4683–4691. [PubMed: 15140939]

Rivera C, Li H, Thomas-Crusells J, Lahtinen H, Viitanen T, Nanobashvili A, Kokaia Z, Airaksinen MS, Voipio J, Kaila K, Saarma M. BDNF-induced TrkB activation down-regulates the K+-Cl-cotransporter KCC2 and impairs neuronal Cl- extrusion. J Cell Biol. 2002; 159:747–752. [PubMed: 12473684]

Ruusuvuori E, Li H, Huttu K, Palva JM, Smirnov S, Rivera C, Kaila K, Voipio J. Carbonic anhydrase isoform VII acts as a molecular switch in the development of synchronous gamma-frequency firing of hippocampal CA1 pyramidal cells. J Neurosci. 2004; 24:2699–2707. [PubMed: 15028762]

Schulte U, Thumfart JO, Klocker N, Sailer CA, Bildl W, Biniossek M, Dehn D, Deller T, Eble S, Abbass K, Wangler T, Knaus HG, Fakler B. The epilepsy-linked Lgi1 protein assembles into presynaptic Kv1 channels and inhibits inactivation by Kvbeta1. Neuron. 2006; 49:697–706. [PubMed: 16504945]

Schwartzkroin PA, Prince DA. Changes in excitatory and inhibitory synaptic potentials leading to epileptogenic activity. Brain Res. 1980; 183:61–76. [PubMed: 6244050]

Sessolo M, Marcon I, Bovetti S, Losi G, Cammarota M, Ratto GM, Fellin T, Carmignoto G. Parvalbumin-Positive Inhibitory Interneurons Oppose Propagation But Favor Generation of Focal Epileptiform Activity. J Neurosci. 2015; 35:9544–9557. [PubMed: 26134638]

Shiri Z, Manseau F, Levesque M, Williams S, Avoli M. Activation of specific neuronal networks leads to different seizure onset types. Ann Neurol. 2016; 79:354–365. [PubMed: 26605509]

Singh B, Ogiwara I, Kaneda M, Tokonami N, Mazaki E, Baba K, Matsuda K, Inoue Y, Yamakawa K. A Kv4.2 truncation mutation in a patient with temporal lobe epilepsy. Neurobiol Dis. 2006; 24:245–253. [PubMed: 16934482]

Somjen GG. Ion regulation in the brain: implications for pathophysiology. Neuroscientist. 2002; 8:254–267. [PubMed: 12061505]

Toyoda I, Fujita S, Thamattoor AK, Buckmaster PS. Unit activity of hippocampal interneurons before spontaneous seizures in an animal model of temporal lobe epilepsy. Journal of Neuroscience. 2015; 35:6600–6618. [PubMed: 25904809]

Traynelis SF, Dingledine R. Potassium-induced spontaneous electrographic seizures in the rat hippocampal slice. J Neurophysiol. 1988; 59:259–276. [PubMed: 3343603]

Uva L, Breschi GL, Gnatkovsky V, Taverna S, de Curtis M. Synchronous inhibitory potentials precede seizure-like events in acute models of focal limbic seizures. J Neurosci. 2015; 35:3048–3055. [PubMed: 25698742]

Viitanen T, Ruusuvuori E, Kaila K, Voipio J. The K+-Cl cotransporter KCC2 promotes GABAergic excitation in the mature rat hippocampus. J Physiol. 2010; 588:1527–1540. [PubMed: 20211979]

Volman V, Bazhenov M, Sejnowski TJ. Pattern of trauma determines the threshold for epileptic activity in a model of cortical deafferentation. Proceedings of the National Academy of Sciences of the United States of America. 2011a; 108:15402–15407. [PubMed: 21896754]

Volman V, Sejnowski TJ, Bazhenov M. Topological basis of epileptogenesis in a model of severe cortical trauma. J Neurophysiol. 2011b; 106:1933–1942. [PubMed: 21775725]

Watanabe M, Fukuda A. Development and regulation of chloride homeostasis in the central nervous system. Front Cell Neurosci. 2015; 9:371. [PubMed: 26441542]

Wei Y, Ullah G, Schiff SJ. Unification of neuronal spikes, seizures, and spreading depression. J Neurosci. 2014; 34:11733–11743. [PubMed: 25164668]

Yamaguchi S, Rogawski MA. Effects of anticonvulsant drugs on 4-aminopyridine-induced seizures in mice. Epilepsy Res. 1992; 11:9–16. [PubMed: 1563341]

Yekhlef L, Breschi GL, Lagostena L, Russo G, Taverna S. Selective activation of parvalbumin- or somatostatin-expressing interneurons triggers epileptic seizurelike activity in mouse medial entorhinal cortex. J Neurophysiol. 2015; 113:1616–1630. [PubMed: 25505119]

Highlights

- A mechanism for the role of the KCC2 co-transporter in seizure onset is proposed.

- The mechanism relies on inhibition-dependent intracellular chloride accumulation and KCC2 co-transporter activation.

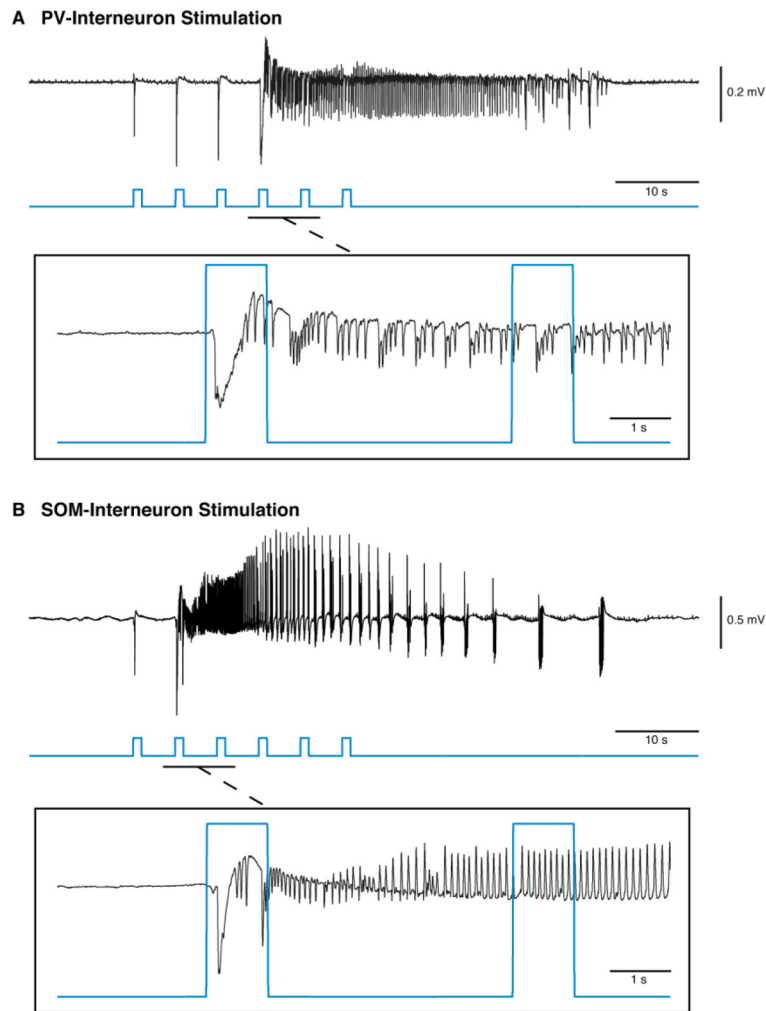- The proconvulsive role of $GABA_A$ involves KCC2 co-transporter activation.

Figure 1.
Ictal discharges can be triggered by optogenetic stimulation of PV- or SOM-positive interneurons. **A**, Ictal discharge evoked by 0.2 Hz series of 1 s light pulses stimulating PV-positive interneurons during bath application of 4AP; ictal onset is expanded to show the timing of the light pulse in relation to ictal onset (box). **B**, The same stimulation parameters applied to SOM-positive interneurons also triggers ictal discharges.
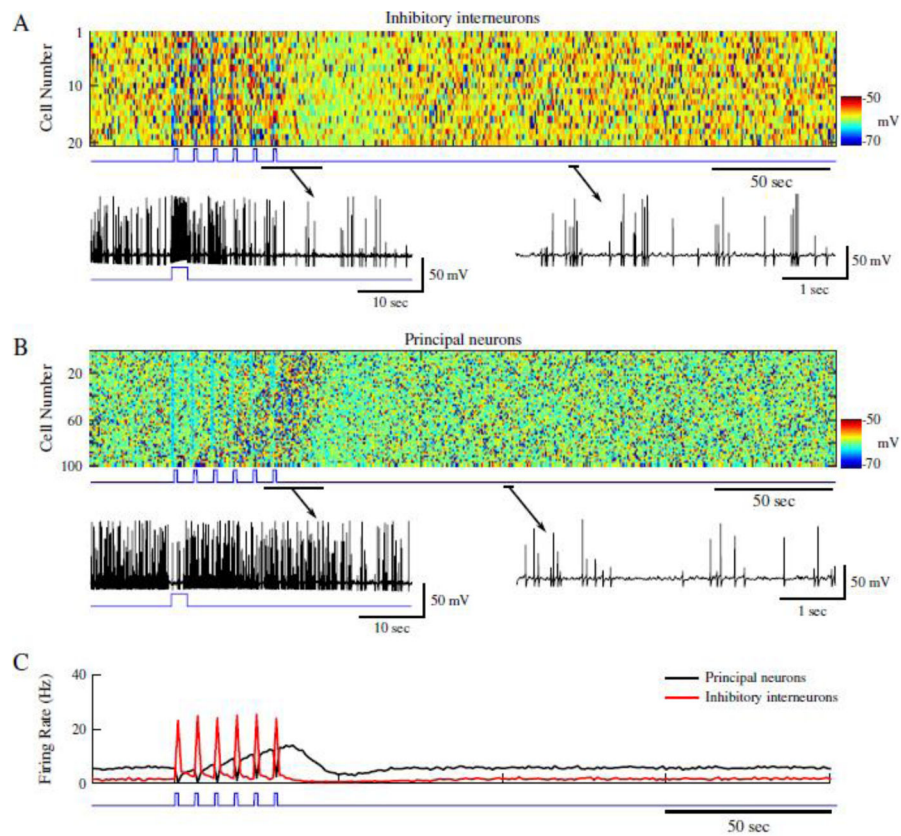
Figure 2.
Stimulation of inhibitory interneurons in a healthy network results in brief silencing of excitatory neurons. **A,** Top panel shows raster plot of interneuron activity. Bottom panel shows zoom in of a single representative interneuron spiking from the network in the top panel. Time of interneuron stimulation is indicated by the blue trace. **B,** Principal neuron network activity with zoom in the spiking pattern of a single principal neuron. The blue trace indicates the time of interneuron stimulation. **C,** Mean firing rates for the interneurons (red) and principal neurons (black).
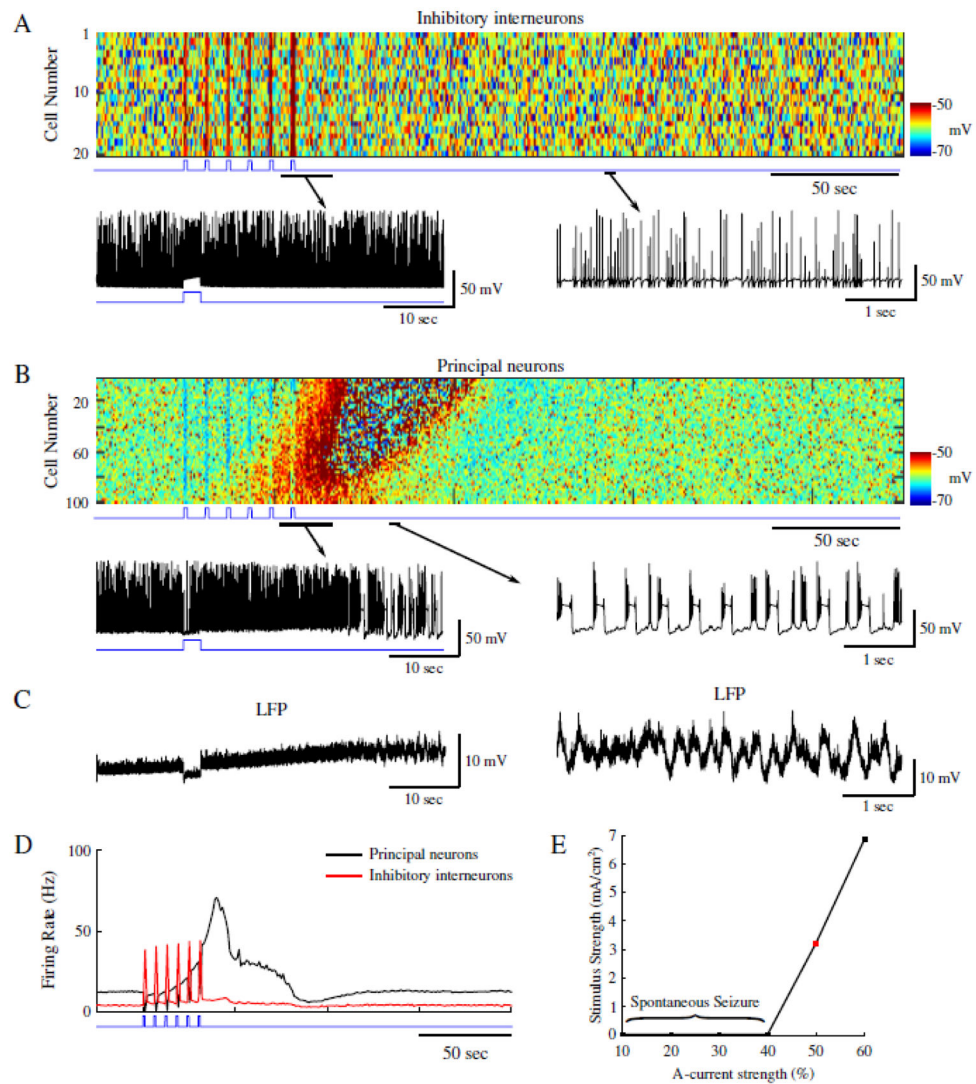
Figure 3.
Reduction of A-current increases network excitability allowing for ictogenesis upon interneuron stimulation. **A,** Top panel shows raster plot of interneuron activity. Bottom panel shows zoom in of a single interneuron spiking from the network in the top panel. Time of interneuron stimulation is indicated by the blue trace. **B,** Principal neuron network activity with zoom in the spiking pattern of a single principal neuron. The blue trace indicates the time of interneuron stimulation. **C,** Corresponding local field potentials (LFP) for the zoom-ins in B. **D,** Mean firing rates for the interneurons (red) and principal neurons (black). **E,** Stimulus strength necessary for seizure generation as a function of A-current strength. Red square indicates the A-current strength used for the network presented in panels A–D.
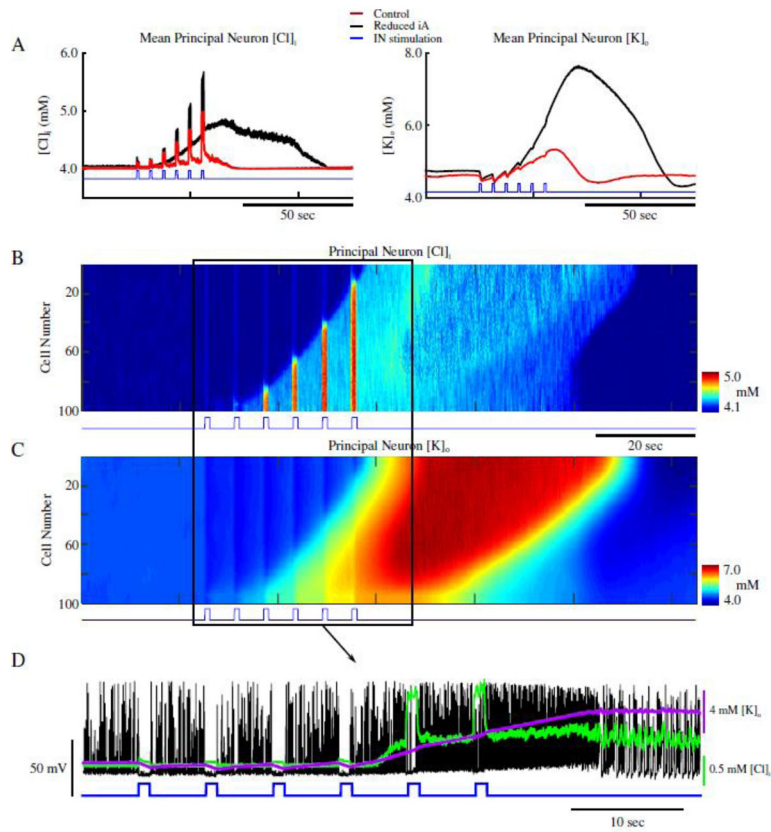
Figure 4.
Increase of $[Cl^-]_i$ leads to gradual accumulation of $[K^+]_o$ and ictogenesis. **A,** Mean $[Cl^-]_i$ (left) and $[K^+]_o$ (right) for principal neurons in the control network from figure 2, and the reduced A-current network in figure 3 (red and black respectively). The blue trace indicates the pattern of interneuron stimulation. **B and C,** network-wide $[Cl^-]_i$ and $[K^+]_o$ for principal neurons. The blue trace indicates the pattern of interneuron stimulation. **D,** Overlay of the spiking of a single principal neuron (black) from figure 3, and the corresponding $[Cl^-]_i$ (green), $[K^+]_o$ (purple), and IN stimulation (blue).
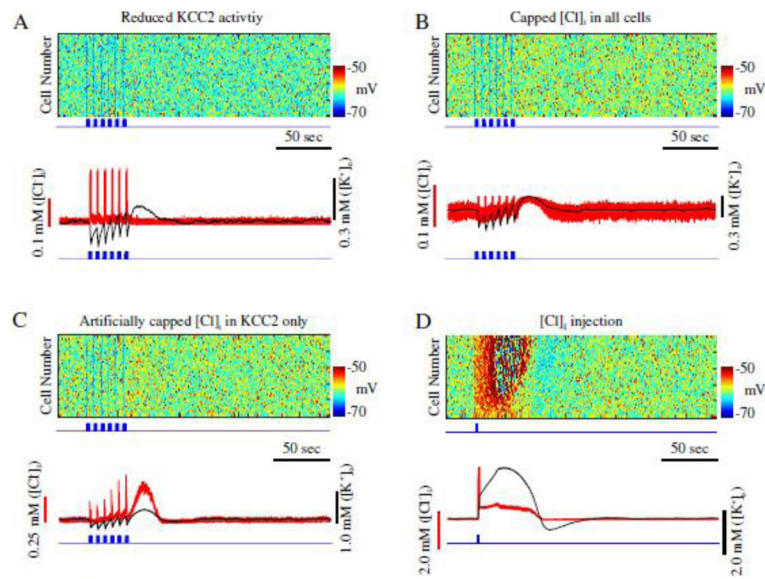
Figure 5.

Seizure onset is dependent on KCC2 activation. **A,** Reduction of KCC2 activity prevents seizure. Top, raster plot of principal neurons in a network with reduced A-current and KCC2 activity. Blue trace indicates pattern of interneurons stimulation. Bottom, corresponding mean $[Cl^-]_i$ (red) and mean $[K^+]_o$ (black) for principal neurons in top panel. **B,** Network with limited $[Cl^-]_i$ accumulation. Top, raster plot showing activity of principal neurons. Bottom, corresponding mean $[Cl^-]_i$ (red) and mean $[K^+]_o$ (black) for principal neurons from the top panel. **C,** Network with artificially impaired $[Cl^-]_i$ sensitive K^+ mechanism. Top, raster plot showing activity of principal neurons. Bottom, corresponding mean $[Cl^-]_i$ (red) and mean $[K^+]_o$ (black) for principal neurons in top panel. **D,** Cl^- injection can trigger seizure. Top, rater showing activity of principal neurons. Blue trace shows time of Cl^- injection to principal neurons. Bottom, corresponding mean $[Cl^-]_i$ (red) and mean $[K^+]_o$ (black) for principal neurons in top panel.
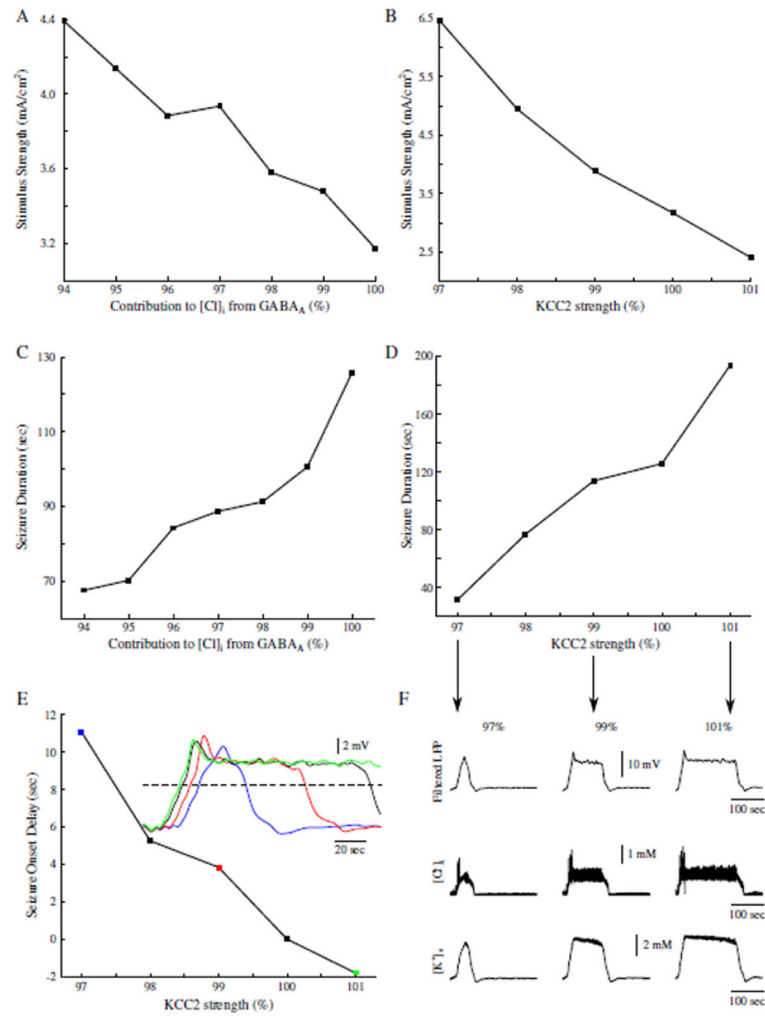
Figure 6.
Contributions to $[Cl^-]_i$ from $GABA_A$, and KCC2 activity modulate seizure threshold, duration and onset. **A,** Seizure threshold as a function of $GABA_A$ contribution to $[Cl^-]_i$. **B,** Seizure threshold as a function of KCC2 strength. **C,** Seizure duration as a function of $GABA_A$ contribution to $[Cl^-]_i$. **D,** Seizure duration as a function of KCC2 activity. **E,** Seizure onset delay as a function of KCC2 activity. Delay was measured between the onset time of a seizure in the control network with 100% KCC2 strength as compared to the seizure onset time in the networks with varied KCC2 strength. Inset shows examples of the filtered seizure LFPs. Colored data points correspond to the sampled data in the inset. Black trace in inset represents the control network with 100% KCC2 activity. Dash line shows threshold used to calculate seizure onset times. **F,** Examples of different seizure durations as a result of varied KCC2 strength. Top, filtered network LFP. Middle and Bottom, corresponding mean $[Cl^-]_i$ and $[K^+]_o$ respectively. Arrows point to the corresponding data points in **D**.